ELSEVIER

Journal of Nuclear Materials 290–293 (2001) 231–237

journal of nuclear materials

www.elsevier.nl/locate/jnucmat

Surface reactions of hydrocarbon radicals: suppression of the re-deposition in fusion experiments via a divertor liner

A. von Keudell [a,*], T. Schwarz-Selinger [a], W. Jacob [a], A. Stevens [b]

[a] *Max-Planck-Institut für Plasmaphysik, EURATOM Association, Boltzmannstr.2, D-85748 Garching, Germany*
[b] *Department of Applied Physics, Eindhoven University of Technology, P.O. Box 513, 5600 MB, Eindhoven, Netherlands*

Abstract

The formation of re-deposited layers consisting of hydrocarbon compounds is of major concern for the development of next-step devices, because the hydrogen bound in these layers contributes to tritium retention in a future fusion reactor. This film formation might be controlled by using a liner in the divertor pump duct to trap or transform neutral growth precursors before they deposit in remote areas of the vacuum vessel. For the understanding of film formation in such a liner the knowledge of sticking coefficients of the growth precursors is mandatory. Therefore, experiments based on the cavity technique were performed to measure surface loss probabilities of hydrocarbon radicals. In addition sticking coefficients of methyl radicals were measured directly applying well-characterized quantified radical beams. To simulate film formation in a liner, a test experiment was performed consisting of a stainless steel tube, which was exposed to a low-temperature plasma from acetylene. The variation of the film thickness along the inner surface of this tube after plasma exposure can be described by a flux comprising of different neutral hydrocarbon radical species using the previously determined sticking coefficients. Suggestions for the control of the formation of re-deposited layers are made and a possible design of such a divertor liner is discussed.

Keywords: Redeposition; Hydrogen retention

1. Introduction

In the present-day fusion experiments, the main ion flux towards the surrounding surfaces impinges onto the divertor, which consists in most cases of graphite tiles in order to withstand the large plasma heat load. This ion flux leads to material sputtering of the surface and formation of volatile reactive neutral hydrocarbons, which may be re-deposited in regions not in direct contact with the plasma in proximity to the divertor [1]. This is of major concern for the development of next-step devices, because these layers consist of hydrocarbon compounds which chemically bind the available H isotopes thus contributing to the tritium retention in a future fusion reactor [2]. These layers are not only found in the divertor, but also in remote areas of the vacuum vessel, where the hydrogen inventory cannot easily be recycled. This leads to a permanent retention of hydrogen isotopes. This problem needs to be mitigated by controlling or suppressing the re-deposition possibly via a proper design of the divertor. Especially a liner inside the pump duct of a divertor can serve as a trap for the hydrocarbon radicals as growth precursors for film formation. The hydrogen inventory in these films inside the liner can then be recycled locally (e.g., by an in situ cleaning discharge or by replacing the liner via remote handling and an external *T*-recovery procedure). In Fig. 1, a sketch of a possible liner structure to be installed at the exit of the divertor is shown: hydrocarbon films are formed at the divertor surface via co-deposition of hydrogen and carbon ions. Depending on the substrate temperature of the divertor and kinetic energy of the ions these co-deposited films are eroded again either via sputtering or via thermal release [3]. The erosion products can be transported across the divertor surface via

* Corresponding author.
E-mail address: von_keudell@ipp.mpg.de (A. von Keudell).

0022-3115/01/$ - see front matter
PII: S0022-3115(00)00435-9

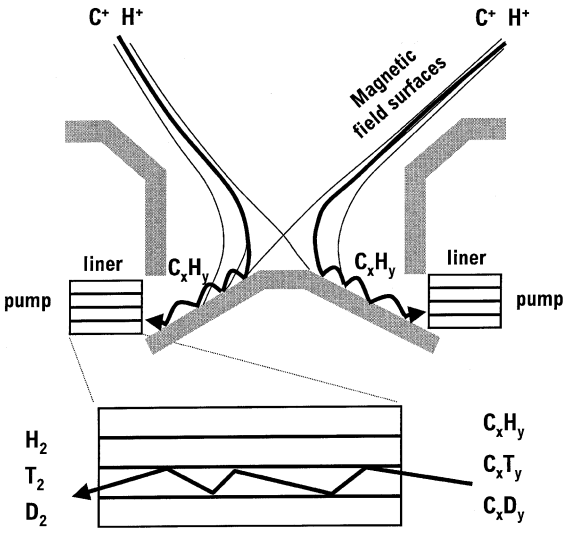

Fig. 1. Sketch of a liner structure in the pump duct of a divertor.

several erosion re-deposition cycles before they reach the liner at the exit of the divertor as neutral C_xH_y species. This liner may consist of an array of tubes in which the hydrocarbon radicals are trapped via film formation, and only stable neutrals like H_2 or CH_4 reach the pump section.

For the design of such a liner, however, an understanding of the underlying mechanism of film formation is mandatory. Some of the key parameters are the sticking coefficients of the different hydrocarbon radicals as the growth precursors. Recently, the surface loss probability β, corresponding to the sum of sticking plus transformation (the probability to react at the surface to a non-reactive volatile product) of various hydrocarbon radicals has been determined by using the cavity technique [3–5]. This yields for sp^1-hybridized precursors like C_2H: $\beta = 0.8, \ldots, 0.9$, and for sp^2-hybridized precursors like C_2H_3: $\beta = 0.35$, and for sp^3-hybridized precursors like CH_3 or C_2H_5: $\beta = 10^{-2}, \ldots, 10^{-3}$. These experiments showed that the surface reactivity scales with the state of hybridization of the growth precursor, which can be explained by different reactivities of the unsaturated hydrocarbons for radical polymerization. With the cavity technique, however, the sticking coefficient itself cannot be measured directly. Therefore, the experiments based on well characterized and absolutely quantified radical beams of atomic hydrogen and methyl (CH_3) were performed. Recently, it was shown that at room temperature, the sticking coefficient of CH_3 at the saturated hydrocarbon film surface is 10^{-4}, whereas it increases by two orders of magnitude to 10^{-2}, if the surface is simultaneously exposed to atomic hydrogen [6].

This paper is divided into three parts. In the first part, the variation of the sticking coefficient of methyl as a function of the radical fluxes onto the film surface is shortly discussed. In the second part, a liner test experiment based on the transport of hydrocarbon radicals in a tube is described. Finally, the consequences for the design of a liner structure in the divertor region of a future fusion experiment are discussed.

2. Experiment

The sticking coefficient of methyl radicals (CH_3), as a dominant precursor for film formation, is measured directly in a radical beam experiment. Quantified radical beams are produced by thermal dissociation of a precursor gas inside a heated tungsten capillary. The dissociation products effuse into an ultra-high vacuum system and interaction of the radicals with the hydrocarbon film surface is monitored in situ via real-time ellipsometry. Two radical sources are implemented, one for methyl radicals producing a flux of 3×10^{14} cm^{-2} s^{-1} and one for atomic hydrogen producing a flux of 4×10^{15} cm^{-2} s^{-1} at the sample surface. Details of the design and performance of the radical sources can be found in [7,8]. The description of the experimental setup to study the radical surface interactions is described in [6,9].

The experimental setup of the liner test experiment is shown schematically in Fig. 2. An electron cyclotron resonance plasma (ECR) from acetylene is used as source for the hydrocarbon radicals. The following external process parameters are chosen: pressure = 0.2 Pa; gas flow = 10 sccm, absorbed microwave power density = 5 kW m^{-3}. Details on the experimental setup and the geometry of the vessel can be found in [10]. A stainless steel tube with a length of 400 mm and an inner diameter of 40 mm is used as the test structure for a 'liner' geometry. This tube is placed at a distance of 200 mm from the resonance zone of the ECR discharge, with the axis of the tube on the symmetry axis of the magnetic field. The whole setup is pumped with a turbomolecular pump and a backing pump with no extra pump system at the end of the test liner. Four cavity samples are inserted in the side wall of the tube. These cavity samples consist of a small box (shown in the inset of Fig. 2) with a silicon substrate as the bottom surface and a silicon substrate as the top surface divided into half leaving a small slit, which is oriented perpendicular to the tube axis facing the inside of the tube. The four cavity samples $C1 \cdots C4$ are placed at 22.3, 82.1, 203.5 and 383 mm from the entrance of the tube, as shown in Fig. 2. Hydrocarbon radicals from the plasma enter these cavity samples via the slit leading to film formation inside. The surface reaction probabilities β can then be deduced ex situ from the characteristic variation of the film thickness inside

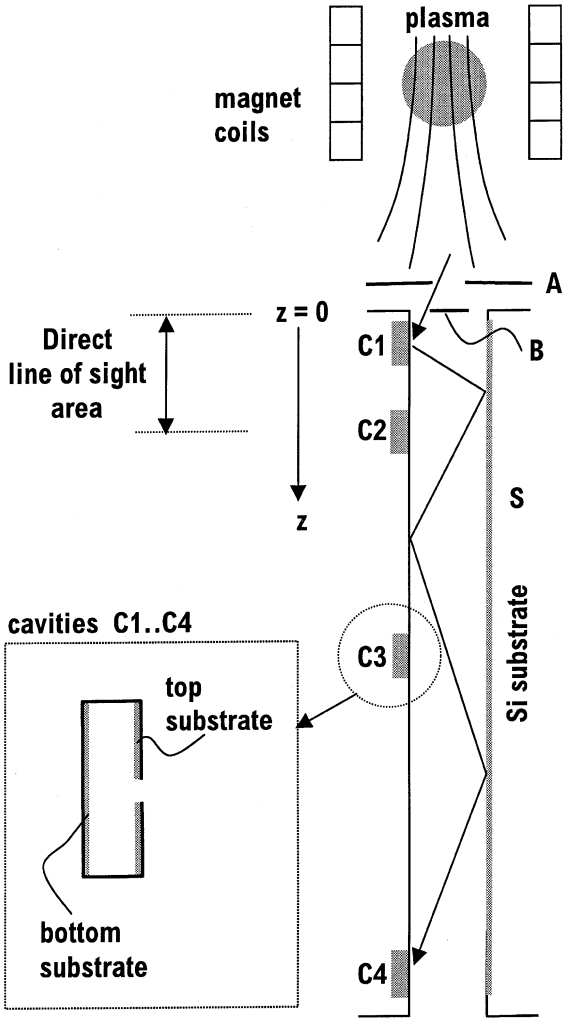

Fig. 2. Sketch of a liner test experiment consisting of a tube exposed to an ECR low-temperature plasma. In this experiment the plasma serves as the source for radicals as precursors for film formation. The tube is equipped with cavity samples C1 ··· C4 inserted in the tube side wall and with silicon substrates S mounted at the inside along the tube. The direct line-of-sight to the plasma is limited to the first 80 mm via a space filter consisting of apertures A and B. The inset shows a sketch of the cavity samples consisting of a box with a silicon substrate as the bottom surface and a silicon substrate as the top surface divided into half.

the cavity sample [5]. Finally, silicon substrates are also inserted in the inner wall (S in Fig. 2) to measure the deposited film thickness at the inner wall along the tube.

It is possible to describe the transport of hydrocarbon radicals inside the tube by consecutive adsorption–desorption cycles of the growth precursors at the inner walls following a cosine angular distribution and ballistic transport between two wall collisions (any gas-phase scattering of the hydrocarbon radicals can be neglected because the mean free path of 750 mm is larger than the dimensions of the tube) [5]. However, film formation inside the tube can occur not only from species which reach a specific surface element via several wall collisions but also via direct line-of-sight from the discharge. Since the latter contribution cannot easily be incorporated in a simple model, species in direct line-of-sight from the discharge are blocked by using a space filter at the entrance of the tube, which consists of a disk with a central hole of 20 mm diameter (part A in Fig. 2) and a second smaller disk with an outer diameter of 24 mm on the axis of the tube and located 20 mm beneath the first disk (part B in Fig. 2). The space filter assures that only the first 80 mm of the inner surface of the tube are in direct line-of-sight from the discharge.

The liner test experiment is performed as follows. First, clean silicon substrates are mounted at the inner walls of the tube and inside the cavity samples. Second, the tube is exposed to an acetylene discharge for 24 h. Finally, the deposited films on the silicon substrates S and inside the cavity samples C1 ··· C4 are analyzed ex situ by ellipsometry. Details on the analysis of the samples and the corresponding modeling of the variation of the film thickness inside the cavity samples can be found in [5].

3. Results and discussion

3.1. Sticking coefficient of methyl

Recently, the interaction of methyl radicals and atomic hydrogen with the surface of hydrocarbon films was measured directly using quantified radical beams [6,9]. It was shown that CH_3 radicals have a sticking coefficient of $s(CH_3) = 10^{-4}$. If, however, an atomic hydrogen beam reacts simultaneously with the film surface, the sticking coefficient for methyl rises to $s(CH_3|H) = 10^{-2}$. The variation of the growth or etch rate at different relative fluxes of the CH_3 and H radical beams impinging on a hydrocarbon film at a substrate temperature of 320 K is shown in Fig. 3. Three regimes can be distinguished: in regime 1, only the atomic hydrogen beam is on, leading to steady-state erosion, corresponding to an erosion yield of 3×10^{-4}. This is in agreement with the known yield for chemical erosion at 320 K [11]. In regime 2, the CH_3 radical beam and the H beam impinge simultaneously onto the surface leading to a steady-state film growth corresponding to a sticking coefficient of $s(CH_3|H) = 10^{-2}$. In regime 3, the H radical beam is switched off and the film growth from CH_3 radical adsorption alone yields to a sticking coefficient of $s(CH_3) = 10^{-4}$. This growth synergism between H and CH_3 can be explained as follows [9]: the incoming flux of atomic hydrogen leads to a steady-state coverage of dangling bonds at the surface via the balance between

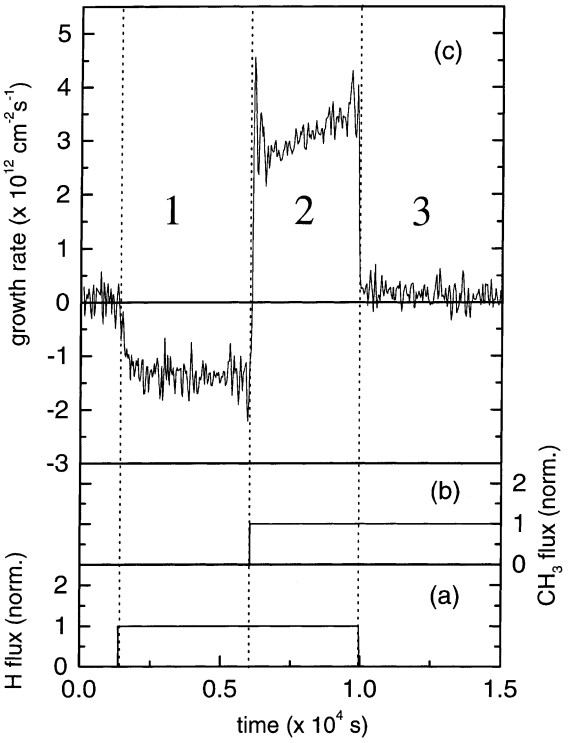

Fig. 3. Variation of the growth or etch rate during exposure of a hydrocarbon film to a CH_3 radical beam and an H radical beam. (a) H flux normalized to 4×10^{15} cm^{-2} s^{-1}; (b) CH_3 flux normalized to 3×10^{14} cm^{-2} s^{-1}; (c) growth/etch rate in incorporated/released carbon atoms.

abstraction and addition of surface bonded hydrogen. At these dangling bonds, the incoming CH_3 radicals can adsorb. If the atomic hydrogen beam is switched off, dangling bonds can only be created by abstraction of surface bonded hydrogen from incoming CH_3, which has a much smaller cross-section compared to abstraction of surface bonded hydrogen by H.

This experiment illustrates that the sticking coefficient for CH_3 strongly depends on the steady-state coverage of dangling bonds at the film surface. The formation of dangling bonds can be caused by abstraction reactions from atomic hydrogen, but also via displacement of surface bonded hydrogen due to the incoming ions or via electron stimulated desorption. The existence of such a growth synergism is in agreement with predictions in the literature [12,13] and measurements of the decay of the CH_3 radical density in the afterglow of a pulsed rf discharge [14].

3.2. Liner test experiment

As a simple test geometry for a divertor liner, the film deposition resulting from hydrocarbon radicals inside a tube is studied. This tube is exposed to a hydrocarbon discharge as the source for hydrocarbon radicals. Fig. 4 shows the deposited film thickness inside the tube after exposure to an acetylene discharge for 24 h. A similar result is found for exposing the tube to a methane discharge. This similarity is due to the fact that in both cases the same hydrocarbon radicals like CH_3, C_2H, C_2H_3, C_2H_5 although in different abundances contribute to the radical flux emanating from the plasma, as estimated from mass spectrometry [15]. For an interpretation of the film deposition along the tube's inner surface, two sections of the tube need to be distinguished. In Section 1, within a distance of 80 mm from the entrance of the tube, the variation of the film thickness is dominated by the incoming flux of radicals and ions from the discharge, since this surface area is in direct line-of-sight from the discharge. In Section 2, the film deposition is dominated by the transport of hydrocarbon radicals inside the tube via consecutive adsorption–desorption cycles. The variation of the film thickness with the distance z from the tube entrance can be described by an exponential decay composed of two decay lengths $z_1 = 30$ mm and $z_2 = 3500$ mm. [1] The presence of an exponential decay of the film thickness with respect to the distance z from the entrance of the tube can be explained as follows: the transport of species from a position z to a position $z + \Delta z$ in the tube can be modeled by reflection of an impinging radical flux $\Phi(z)$ at the position z. The reflected species contribute to the impinging radical flux $\Phi(z + \Delta z)$ at position $z + \Delta z$. Thereby, the flux $\Phi(z + \Delta z)$ towards the inner wall at position $z + \Delta z$ is proportional to the flux $\Phi(z)$ at position z times a reflection coefficient r. This leads to the functional behavior of an exponential decay of $\Phi(z)$ with respect to the distance from the entrance of the tube, which can be converted to a variation of the deposited film thickness d via $d(z) = \Phi(z) \times s$ using the sticking coefficient s.

The observation of an exponential decay of the film thickness inside the tube comprising of two decay lengths can be explained by the contribution of two different groups of growth precursors to the film formation. Precursors with a large β are trapped close to the entrance of the tube, whereas precursors with small β survive many wall collisions before they adsorb at remote positions along the tube. This leads to a variation of the impinging radical flux with respect to the distance z from the tube entrance. The relative contribution of

[1] In general, it is possible to model the film formation inside the tube via consecutive adsorption–desorption cycles similar to the model as presented in [6] This requires, however, atomically flat inner surfaces of the tube-like silicon substrates instead of the stainless steel surface, in order to use a simple cosine law to describe the angular distribution of the desorbing species.

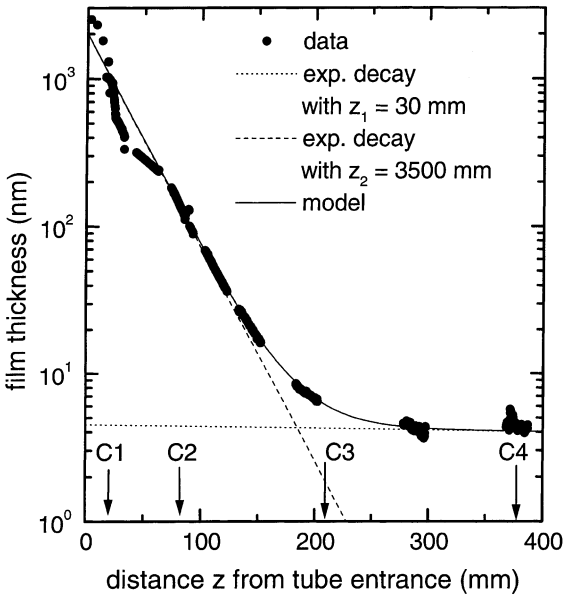

Fig. 4. Decrease of the film thickness with respect to the distance z from the tube entrance. Modeling via an exponential decay consisting of two decay lengths $z_1 = 30$ mm and $z_2 = 3500$ mm. The positions of the cavity samples are marked with C1 $\cdots$ C4.

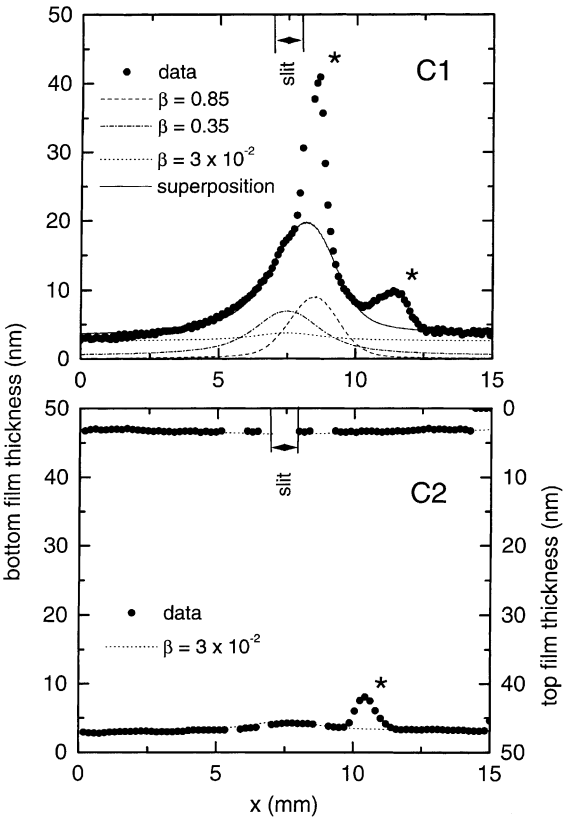

Fig. 5. Deposition profiles in cavities C1 and C2 after exposure of the tube to an acetylene discharge for 24 h. Modeling of the deposition profile with the superposition of three surface loss probabilities $\beta_1 = 0.85$, $\beta_2 = 0.35$, and $\beta_3 = 3 \times 10^{-2}$.

different growth precursors to the radical flux at a position z can be monitored by using cavity samples at various positions inside the tube. The analysis of the deposition profile inside the cavity samples reveals the presence of different precursors for film formation as identified by their individual surface loss probabilities β [5].

The positions of the cavity samples C1 $\cdots$ C4 are marked in Fig. 4. Film deposition was found in cavities C1 and C2, whereas no film deposition was detectable in cavities C3 and C4 within the resolution accuracy of the film thickness measurement ($\sim$2 nm) via ellipsometry. The film thickness variation in the cavities C1 and C2 is shown in Fig. 5. The deposition profiles in the cavities are modeled via a superposition of the contributions from precursors with different surface loss probabilities β as described in [5]: $\beta = 0.85$ for sp^1-hybridized precursors, $\beta = 0.35$ for sp^2-hybridized precursors and $\beta = 3 \times 10^{-2}$ for sp^3-hybridized precursors. It can be seen that the deposition profile at the bottom of C1 is in agreement with the superposition of three β values, whereas the deposition profile in C2 can be modeled by using only a single β value of 3×10^{-2}. In addition, the center of the peak corresponding to $\beta = 0.85$ is shifted from the symmetry axis of the cavity C1, which is due to the fact that the main flux of incoming radicals impinge at an oblique angle of incidence onto the cavity sample (see Fig. 2) leading to a lateral shift of the deposition profiles for large β values. Furthermore, additional peaks are observed in the deposition profiles of the bottom surface in the cavities C1 and C2 (marked with $*$ in Fig. 5). This can be explained by film growth due to adsorption of species with a sticking coefficient close to unity since no similar peaks can be found at the top deposition profile (see deposition profile in cavity C2 in Fig. 5). These species might originate directly from a sputtering of the re-deposited films at the slit entrance by incoming ions in direct line-of-sight from the discharge. The contribution of these species to the interpretation of the deposition profiles is not considered in the analysis. Finally, no film deposition is found at the top surface of C1, which can be explained by the thermally activated re-etching due to atomic hydrogen: the top surface consists of a free standing silicon wafer, which is in direct line-of-sight to the plasma in case of cavity C1. Therefore, this top wafer is efficiently heated by the plasma and the thermally activated re-etching by atomic hydrogen prevents film formation on this silicon wafer [16]. The bottom substrate of C1 and the silicon substrates in C2 $\cdots$ C4, however, are exposed to a much

lower heat load and the corresponding low substrate temperature prevents the re-etching of the films by atomic hydrogen.

This shows that hydrocarbon radicals with a large surface loss probability $\beta > 0.3$ are efficiently trapped in Section 1 of the test liner. Furthermore, one can conclude that the film growth in Section 2 with an exponential decay length of $z_1 = 30$ mm is caused by species with a β value of 3×10^{-2}. The absolute value of this surface loss probability is consistent with a sticking coefficient of 10^{-2} for the adsorption of sp^3 growth precursors like CH_3 on a hydrocarbon film surface *with* an additional flux of atomic hydrogen. This implies, however, a significant contribution of atomic hydrogen to the radical flux impinging onto the inner wall of the tube within the measured decay length of $z_1 = 30$ mm. This will be discussed further below.

Based on the known cross-sections for abstraction of surface bonded hydrogen due to incoming atomic hydrogen ($= 0.05$ Å^2) and for addition of incoming hydrogen to a dangling bond at the surface ($= 1.3$ Å^2) [11], a surface loss probability for H of $\beta(\mathrm{H}) = 1.4 \times 10^{-2}$ can be deduced. A detailed analysis of the growth synergism between H and CH_3 indicates that the growth rate is CH_3 flux limited for a large hydrogen flux with respect to the CH_3 flux and H flux limited for a comparable or smaller H flux with respect to the CH_3 flux [9]. If the synergistic film growth inside the tube is H flux limited, as will be shown below, the growth rate is proportional to the H flux and the variation of the film thickness corresponds thereby to a quantity proportional to the local H flux. The same argument can be applied for the interpretation of the surface loss probability β, since it is also derived from the variation of the film thickness along the tube. In this view, the observation of $\beta = 3 \times 10^{-2}$ in the cavity C2, as well as the short decay length of $z_1 = 30$ mm are a measure for the surface loss of atomic hydrogen and not for the loss of methyl radicals. The sticking coefficient of CH_3 determines only the absolute value of the film thickness within the decay length z_1, whereas the slope of the decay is determined by $\beta(\mathrm{H})$.

A decay length of $z_2 = 3500$ mm is consistent with film formation due to the adsorption of sp^3-hybridized growth precursors on a saturated hydrocarbon film surface with a sticking coefficient of $s = 10^{-4}$. This is characteristic for adsorption on a hydrocarbon film surface *without* an additional flux of atomic hydrogen. From the cross-sections for CH_3 adsorption at a dangling bond (3.8 Å^2) and for abstraction of surface bonded hydrogen due to incoming CH_3 (1.5×10^{-3} Å) [9], a surface loss probability $\beta(CH_3) = 2.2 \times 10^{-4}$ can be deduced. Therefore, the difference in the decay lengths of $z_1 = 30$ mm and $z_2 = 3500$ mm is in reasonable agreement with the difference in surface loss probabilities of $\beta(\mathrm{H}) = 1.4 \times 10^{-2}$ and $\beta(CH_3) = 2.2 \times 10^{-4}$. The fact that the film deposition which occurs in Section 2 (see Fig. 2) with the long decay length is dominated by adsorption of CH_3 leads to the conclusion that the impinging CH_3 flux at the beginning of Section 2 is larger compared to the H flux, since otherwise CH_3 would be completely consumed within the short decay length of $z_1 = 30$ mm and no deposition with a long decay length would be visible. This verifies the above-mentioned assumption that the synergistic growth is H flux limited.

Based on this interpretation, the decrease of the film thickness with the distance from the tube entrance can be divided into three regions: (i) species with a surface loss probability $\beta > 0.3$ are trapped in Section 1 of the tube which corresponds mainly to the region in direct line-of-sight from the plasma; (ii) sp^3-hybridized precursors are trapped within a decay length of $z_1 = 30$ mm at the beginning of Section 2 with a sticking coefficient of $\sim 10^{-2}$ due to the growth synergism caused by the simultaneous interaction with atomic hydrogen at the film surface; finally (iii), sp^3-hybridized precursors, which survive the wall collisions in regions (i) and (ii) are trapped within a decay length of $z_2 = 3500$ mm with a sticking coefficient of 10^{-4} since the contribution of atomic hydrogen to the impinging radical flux onto the inner wall is already consumed in region (ii).

3.3. Consequences for the design of a divertor liner

The so-called 'liner test experiment', which consisted of investigating the transport of hydrocarbon radicals along the wall of a tube showed that species with different sticking coefficients contribute predominantly to film growth in different regions with respect to the tube entrance. Very reactive species like sp^1- and sp^2-hybridized growth precursors have a large sticking coefficient and are efficiently trapped close to the tube entrance. Less reactive species, like sp^3 growth precursors, have a sticking coefficient of $\sim 10^{-2}$ in the case of an additional atomic hydrogen flux towards the surface and are trapped in the tube within a decay length in the range of centimeters. Therefore, a tube with an aspect ratio of $A \sim 10$ (i.e., $A = L/D$ with $L =$ tube length and $D =$ tube diameter) is sufficient to trap the hydrocarbon radicals, which have a large sticking coefficient. However, species with a very low reactivity, which survive the wall collisions in the section of the tube necessary for consuming the contribution of atomic hydrogen, will have in the following section a sticking coefficient of $\sim 10^{-4}$ corresponding to a decay length in the range of meters. A tube with an aspect ratio of $A \sim 100, \ldots, 1000$ would in this case be required, because the hydrocarbon radicals undergo in such a tube many wall collisions resulting in a large combined probability for the occurrence of a loss process at the inner wall. The absolute contribution of the low reactive species to the formation of re-deposited film inside the tube is only in the range of

10^{-3} in a tube of 400 mm length, as can be estimated from the variation of the film thickness as shown in Fig. 4. However, these species will survive many wall collisions even after leaving the liner structure at the back end and might be transported over large distances to very remote areas of the vacuum vessel where they still can contribute to film growth.

Based on these results, the following suggestions can be made for a divertor liner. The trapping of species with a sticking coefficient larger than 10^{-2} can be efficiently achieved by using for example a tube system with an aspect ratio of 10 and an obstruction at the entrance to prevent direct line-of-sight transmission of the radicals. The trapping of species with a smaller sticking coefficient requires, however, larger aspect ratios in the range 100–1000 or porous filters to increase the number of wall collisions. Any severe obstruction inside a liner like a porous filter would, however, deteriorate drastically the pump efficiency. Alternatively, the liner surface might be activated in order to assure a sticking coefficient above 10^{-2} for all precursors of film formation. This can be realized for example by an additional supply of atomic hydrogen behind the liner, which creates dangling bonds on the surrounding surfaces serving as adsorption sites for the low reactive sp^3 growth precursors. This surface activation might also be realized via an additional heating or via an additional ion bombardment. The exact implementation of these design suggestions and the necessary process parameters will be the subject of future experiments.

4. Conclusion

The use of a so-called liner in the divertor of future fusion experiments can significantly reduce the formation of re-deposited layers in remote areas of the vacuum vessel. This liner can consist of an array of tubes between the divertor and the pump duct in which the growth precursors for film formation are trapped. The transport of hydrocarbon radicals through a tube was studied by exposing the tube to a hydrocarbon discharge as an efficient source for hydrocarbon radicals. From the variation of the re-deposited film thickness along the inside of the tube and from the deposition profiles inside the cavity samples inserted along the wall, it was concluded that different growth precursors are trapped in different regions with respect to the tube entrance. Species with a high sticking coefficient $s > 10^{-2}$ are trapped in a region of the tube corresponding to an aspect ratio of 10. Species with a low sticking coefficient in the range of 10^{-4} require aspect ratios of the tube in the range of 100 or higher. This aspect ratio, however, might be lowered by enhancing the sticking coefficient at the inner wall of the whole tube via generating an additional flux of atomic hydrogen behind the liner.

References

[1] P. Andrew, D. Brennan, J.P. Coad, J. Ehrenberg, M. Gadeberg, A. Gibson, M. Groth, J. How, O.N. Jarvis, H. Jensen, R. Lässer, F. Marcus, R. Monk, P. Morgan, J. Orchard, A. Peacock, R. Pearce, M. Pick, A. Rossi, B. Schunke, M. Stamp, M. von Hellermann, D.L. Hillis, J. Horgan, J. Nucl. Mater. 266–269 (1999) 153.
[2] G. Federici, R. Anderl, J.N. Brooks, R. Causey, J.P. Coad, D. Cowgill, R. Doerner, A. Haasz, G. Longhurst, S. Luckhardt, D. Mueller, A. Peacock, M. Pick, C.H. Skinner, W. Wampler, K. Wilson, C. Wong, C. Wu, D. Youchison, Fus. Eng. Des. 39–40 (1998) 445.
[3] A. von Keudell, C. Hopf, T. Schwarz-Selinger, W. Jacob, Nucl. Fus. 39 (1999) 1451.
[4] C. Hopf, K. Letourneur, W. Jacob, T. Schwarz-Selinger, A. von Keudell, Appl. Phys. Lett. 74 (1999) 3800.
[5] C. Hopf, T. Schwarz-Selinger, W. Jacob, A. von Keudell, J. Appl. Phys. 87 (2000) 2719.
[6] A. von Keudell, T. Schwarz-Selinger, M. Meier, W. Jacob, Appl. Phys. Lett. 76 (2000) 676.
[7] T. Schwarz-Selinger, A. von Keudell, W. Jacob, J. Vac. Sci. Technol. A 18 (2000) 995.
[8] T. Schwarz-Selinger, V. Dose, W. Jacob, A. von Keudell, J. Vac. Sci. Technol. A, to be published.
[9] A. von Keudell, T. Schwarz-Selinger, W. Jacob, J. Appl. Phys. (submitted).
[10] B. Landkammer, A. von Keudell, W. Jacob, J. Nucl. Mater. 264 (1999) 48.
[11] J. Küppers, Surf. Sci. Rep. 22 (1995) 249.
[12] A. von Keudell, W. Möller, R. Hytry, Appl. Phys. Lett. 62 (1993) 937.
[13] W. Möller, W. Fukarek, K. Lange, A. von Keudell, W. Jacob, Jpn. J. Appl. Phys. 34 (1995) 2163.
[14] M. Shiratani, J. Jolly, H. Videlot, J. Perrin, Jpn. J. Appl. Phys. 36 (1997) 4752.
[15] T. Schwarz-Selinger, A. von Keudell, W. Jacob, J. Appl. Phys. 86 (7) (1999) 1.
[16] A. von Keudell, W. Jacob, J. Appl. Phys. 79 (1996) 1092.